

Solar and Stellar Flares

L Doyle^{1,2}, G Ramsay¹, J.G. Doyle¹, P. Wyper³, E. Scullion², K. Wu⁴
and J. A. McLaughlin²

¹Armagh Observatory, College Hill, Armagh, BT61 9DG, UK

²Mathematics, Physics and Electrical Engineering, Northumbria University, Newcastle upon Tyne, NE1 8ST, UK

³Department of Mathematical Sciences, Durham University, Durham, DH1 3LE, UK

⁴Mullard Space Science Laboratory, University College London, Holmbury St Mary, Surrey RH5 6NT

Abstract. We report on our project to study the activity in both the Sun and low mass stars. Utilising high cadence, H α observations of a filament eruption made using the CRISP spectro polarimeter mounted on the Swedish Solar Telescope has allowed us to determine 3D velocity maps of the event. To gain insight to the physical mechanism which drives the event we have qualitatively compared our observation to a 3D MHD reconnection model. Solar-type and low mass stars can be highly active producing flares with energies exceeding 10^{33} erg. Surprisingly we find no correlation between the number of flares and the rotation phase, since we would expect more flares at flux minimum when the dominant starspot is most visible. We outline four scenarios to explain our finding: polar spots, stellar binarity, the presence of orbiting planets and multiple spot locations. Our solar flare model can be used to aid our understanding of the origin of flares in other stars. By scaling up our solar model to replicate energies seen in the stellar flares we aim to investigate the conditions needed for such high energy flares.

Keywords. Sun: chromosphere, Sun: flares, stars: low-mass, stars: flare

1. Introduction

Solar flares represent a sudden increase in radiation which results from a rapid reconfiguration of the coronal magnetic field. These events are extremely powerful and are observed across the entire electromagnetic spectrum, possessing energy outputs up to 10^{32} erg (Fletcher *et al.* 2011). Magnetic energy released from solar flares can be observed as multiple phenomena including flare ribbons and post-flare arcades, but also in filament eruptions (e.g. Schmieder *et al.* 2013), coronal mass ejections (CME's) (Karpen *et al.* 2012) and blow-out jets (e.g. Young & Muglach 2014). Overall, the pre-flare magnetic topology is responsible for determining which of these phenomena will manifest to produce a solar flare.

In addition to solar flares, stellar flares have been observed on stars similar to the Sun and less massive stars over many decades with energies exceeding 10^{33} erg (e.g. Schaefer *et al.* 2000). Known as 'superflares' these large outbursts can have severe consequences for any orbiting planets atmosphere, therefore, understanding their frequency and origin is vital for the existence of life. Solar-type stars have a similar interior structure to our Sun, yet they possess stronger magnetic fields producing higher levels of activity and stronger flares (Maehara *et al.* 2012). In low-mass stars with spectral types later than M4, their interiors are thought to be fully convective (Hawley *et al.* 2014) so they possess no tachocline (the boundary between the radiative and convective zones) and must generate their magnetic fields through a different dynamo mechanism. However, despite this, these stars can also show increased levels of flaring activity with flares reaching energies much greater than our Sun.

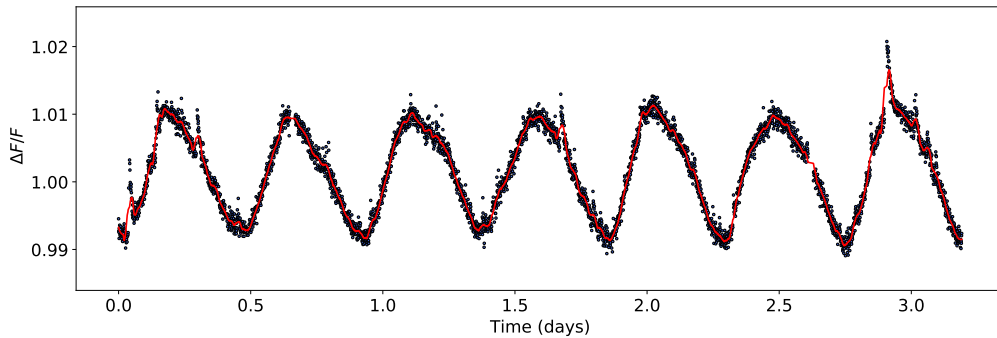


Figure 1. A section of the K2 lightcurve for the known flare star GJ 3225 (EPIC 210758829) which covers ~ 3 days. This star has a spectral type of M4.5 and rotation period, P_{rot} , of 0.45 days. The black points represent the K2 data points which have a cadence of 1 min and the red line is the Savitzky-Golay filtered, smoothed data.

As the Sun is our nearest star we are able to collect detailed spatial observations of its many phenomena from large scale flares and CME’s to the smaller scale granulation and spicules. In addition, there are historical data including spot observations and number, and since the launch of the Solar Dynamics Observatory in 2010 the Sun is observed 24/7. Along with all of these observations comes a deep knowledge and understanding of the mechanisms which are at play on our nearest star and how they can affect the Earth and Solar System. In stellar physics, although the number of stars now observed by missions such as Kepler, TESS and Gaia is nearing 2 billion, the lack of detailed and long-term observations remains an issue. The capabilities of our technology and the vast distances between us and our neighbouring stars restricts our ability to produce observations which show details of the magnetic activity. Therefore, we should be looking to use the knowledge gained from detailed solar observations to illuminate our understanding of stellar flares. In this paper, we look at the solar-stellar flare connection through detailed observations of a confined solar flare event and use the results to provide insights into large scale flare events observed on other stars.

2. Stellar Flare Studies

The brightness of many stars show periodic changes as they rotate. This is widely thought to be the result of a large dominant starspot which is cooler than its surroundings moving in and out of view as the star rotates (see Figure 1). From observations of the Sun, we know flares typically originate near sunspots so it is natural to expect flares to originate from starspots in other stars. If the analogy between solar and stellar flares holds, then we would expect to see a correlation between the timing of stellar flares and flare numbers.

The relationship between sunspots and flares in solar physics has been studied for decades with both of these phenomena being closely linked. For example, Guo *et al.* (2014) used flares from solar cycles 22 and 23 to compute a statistical study on the dependence of flares with sunspots and rotational phase. Overall, they found X-class flares were in phase with the solar cycle, suggesting flares follow the same 11 year cycle as sunspots. In a sample of solar-type stars Maehara *et al.* (2017) looked at the correlation between starspots and superflares using Kepler data, finding the superflares tend to originate from regions which hosted larger spots.

Despite the comprehensive work on stellar flares over the years, one area which has

not been studied in great detail is the correlation between stellar flares and starspots. In these next sections we go on to look at the work we have carried out on the rotational phase dependency of stellar flares in multiple samples of both low mass and solar-type stars.

2.1. Low Mass Stars

Over the course of nine years, Kepler/K2 has provided a wealth of photometric observations for over half a million stars revolutionising the field of stellar physics. In our initial study Doyle *et al.* 2018 (henceforth Paper 1), we utilised K2 short cadence 1-min data from Fields 1 - 9 to conduct a statistical analysis of the flares on 34 M dwarfs. Our stellar sample ranged in spectral type from M0 - L1 and mass from $0.58M_{\odot}$ - $0.08M_{\odot}$. Each target was observed for ~ 70 - 80 days producing a near continuous lightcurve over this period, additionally the short cadence (1-min) data is of great importance as it allows for the detection of flares with durations within a few minutes, providing a more comprehensive view of the stellar activity.

We derive rotation periods for each of the stars in our sample using the rotational modulation within the lightcurve. We utilise a Lomb-Scargle (LS) periodogram to determine the rotation period, P_{rot} and define phase zero, ϕ_0 , as the minimum of the rotational modulation. Once complete, we looked to identifying and cataloging all flares in each of our targets. To do this we used an IDL suite of programs called FBEYE (see Davenport (2014) for more details). This program produces a comprehensive list of all flares and their properties in each star including start, peak and end times, flux peak, and equivalent duration. All of the flares were manually checked by eye to validate their nature. Next, the energies of the flares are calculated within the Kepler bandpass as the quiescent luminosity, L_* , multiplied by the equivalent duration (area under flare lightcurve). We used PanStarrs (Chambers *et al.* 2016) magnitudes in the g, r, i and z bands to construct a template spectrum of each star and convolved it with the Kepler bandpass, deriving the quiescent flux of the stars. The quiescent luminosity is then calculated by multiplying the flux by $4\pi d^2$, where the distance, d has been determined from Gaia DR2 (Gaia Collaboration *et al.* 2016) parallaxes.

We can now go on to investigate the rotational phase of the flares and determine whether there is a preference for certain rotational phases. For this analysis we can only use stars which possess rotation periods shorter than the observation length and as a result 8 of our targets were omitted from further analysis. In order to test whether the phase distribution of the flares is random within our M dwarf sample we utilise a simple χ^2_{ν} statistical test. For this, flares were split into low and high energy with a cut-off determined by the median energy and rotational phase was split into 10 bins. The χ^2_{ν} was determined for each star in the all, low and high energy flare categories, where the degrees of freedom, ν , is 9. These results showed there was no preference for any rotational phase within all of the stars individually suggesting the flares do not originate from the large starspot producing the rotational modulation. This result comes as a surprise as it goes against where we believe flares should originate from.

Kepler's successor, the Transiting Exoplanet Survey Satellite (TESS: Ricker *et al.* 2015) was launched in April 2018 and has since been making observations of the northern hemisphere as part of its 2-year prime mission. Unlike Kepler/K2, TESS makes month long observations at 2-min cadence of stars brighter than ~ 13 mag. In our second study, Doyle *et al.* (2019) (henceforth Paper 2), we use TESS short cadence 2-min photometric data from a sample of 149 M dwarfs made in Sectors 1 - 3. In Paper 1 we calculate the rotation periods, quiescent luminosity of the stars and identify all flares determining the energies for each. For Paper 2 using TESS data, we use the same methods as Paper 1,

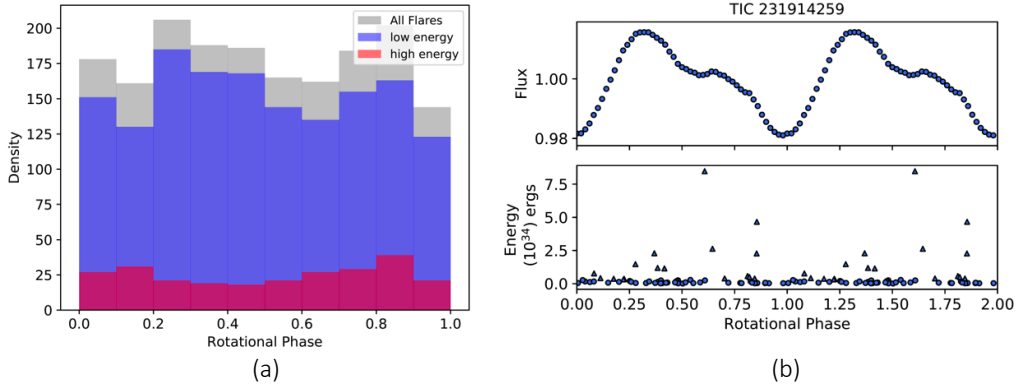


Figure 2. Panel (a) is the rotational phase distribution for all 1776 flares from the sample of 149 M dwarfs observed with TESS. Panel (b) shows the binned, folded lightcurve with $P_{rot} = 1.43$ days (upper) and the rotational phase distribution of the flares on 2MASS J0030-6236 (lower). The coverage of $\phi = 1.0 - 2.0$ is a repeat of $\phi = 0.0 - 1.0$ and the triangles represent higher energy flares and the circles represent lower energy flares with a cut off of 3.16×10^{33} erg.

however, instead of PanStarrs magnitudes we use SkyMapper (Wolf *et al.* 2018) magnitudes as Sectors 1 - 3 are in the southern hemisphere. We also utilised the same χ^2_ν statistical test to determine whether the distribution of flares within our sample of 149 M dwarfs was random or whether there was a preference for certain rotational phases. Firstly, there was no evidence for a correlation between rotational phase of the flares in any of the 149 stars in our sample. Our χ^2_ν test indicates the flares are randomly distributed and we show the histogram of that distribution in Figure 2(a) where there is a uniform spread in low, high and all energy flares. Similarly, in individual stars, see Figure 2(b), the same χ^2_ν test was also applied and again showed there was no preference for rotational phase within the stars individually.

We highlight 4 scenarios to explain the lack of a correlation between flares and the large starspot on the surface on these stars. Firstly, there is the potential for star-planet interactions (SPI's) causing flaring activity at all rotational phases. Similar to this, there is also the potential for star-star interactions which, like SPI's, would depend on the binary orbital period. A third scenario is the presence of polar spots (Strassmeier 1996) on the surface of these stars interacting with emerging active regions and quiet sun regions as the star rotates. Polar spots are not present on our Sun due to its dynamo mechanism. However, can be present in low-mass stars where the inclination of these stars could be such that these polar spots would be visible at all rotational phases. Lastly, there is the potential for multiple spots locations across the disk of the star. A lightcurve with a one or two spot model does not produce the sinusoidal pattern observed in many low mass stars and if one spot were present on the disk we would always observe flat-top lightcurves. Therefore, the sinusoidal pattern could be produced by multiple active regions hosting spots where, there is one possessing a larger spot/group of spots. In theory, this active region should still produce higher energy flares according to McIntosh (1990) and so, a correlation between flare number and rotational phase should still be observed.

2.2. Solar-Type Stars

We have extended our study of stellar flares using TESS to look at solar-type stars. In this study, we present a statistical analysis of stellar flares on solar-type stars from F7 - K2 spectral type, using photometric data in 2-min cadence from TESS of the whole Northern hemisphere (Sectors 1 - 13). Overall, we have 210 solar-type stars in our sample and have

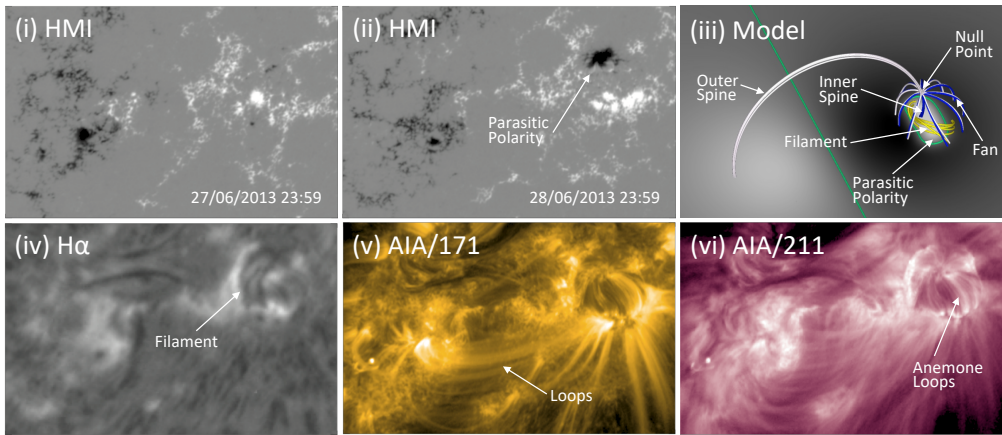


Figure 3. This selection of images shows the active region in multi-wavelengths from GONG, AIA and HMI. Panel (i) and (ii) show the HMI magnetogram before and after the parasitic polarity appears, (iii) shows the pre-flare magnetic field within the simulation and (iv) - (vi) shows the region after the parasitic polarity appears in $H\alpha$, AIA 171Å and AIA 211Å.

identified 1974 flares with energies between $10^{31} - 10^{36}$ erg. We are not only looking at the rotational phase distribution of the flares but also flare occurrence and year-long observations of a handful of stars, monitoring the variability of stellar activity. So far, the preliminary results of this study show no correlation between the rotational phase of stellar flares and flare number. Again, these stars all show rotational modulation as a result of starspots present on the disk so, this result comes as a surprise. As a benchmark, we are using historic GOES data of solar flares to identify the solar rotation and activity cycles to detail the close relationship between solar flares and sunspots. This will in turn help us to understand the relationship between stellar flares and starspots on other stars.

3. The Solar Study

3.1. Observation

Throughout this study we use multi-wavelength observations from the Swedish Solar Telescope (SST: Scharmer *et al.* 2008), Solar Dynamics Observatory (SDO: Pesnell *et al.* 2012) and the Global Oscillations Network Group (GONG: Harvey *et al.* 2011). On the 30th June 2013 in AR 11778 SST/CRISP observed a filament eruption associated with a C1.5 class solar flare. These observations consist of a series of images scanning the $H\alpha$ spectral line in the range of $\pm 1.38\text{\AA}$ resulting in 33 spectral line positions. Overall, this active region was observed for one hour with a temporal resolution of 7.27 seconds where the eruption and flare occurred within the first 5 minutes. Full-Disk-H-alpha (FDHA) images were acquired from GONG and used as context to identify and monitor the filament as it evolves and erupts. Images from SDO/AIA and HMI were also used to provide a larger FOV in comparison to SST and to monitor the development of the active region. In particular we used images from AIA wavelengths 131Å 171Å 211Å and 304Å which represents the chromosphere, transition region, corona and flaring regions.

Figure 3 shows the pre-flare structure of the active region. In panel (i) we see the HMI magnetogram before the emergence of a parasitic polarity (a patch of negative field within a positive region) and (ii) shows the parasitic polarity. Panels (iv) - (vi) then show the FDHA and AIA images of the same time frame as (ii) detailing the filament structure which lies over the parasitic polarity and loop structure within the

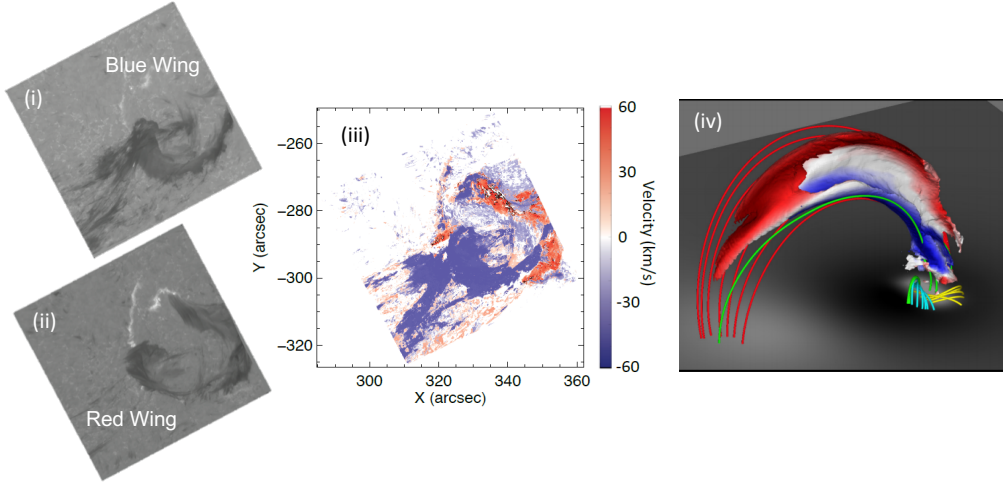


Figure 4. Panels (i) and (ii) shows the SST/CRISP images from both the red and blue wings of the $H\alpha$ absorption profile, panel (iii) is the amalgamated velocity map of the blue and red wings created from Doppler velocities of the SST/CRISP $H\alpha$ profiles and panel (iv) is the model of the eruption with an isosurface of velocity to show the jet.

active region. Panel (iii) then shows the corresponding pre-flare magnetic field structure of the 3D MHD simulation showing the structures observed within the multi-wavelength observations. After this time the parasitic polarity begins to break down and disperse which is followed by the eruption of the filament. During the eruption brightenings are observed in AIA 171Å adjacent to the filament in loops and underneath the filament as it erupts, all of which are signatures of magnetic reconnection. Once the filament erupts it propagates eastwards as a helical jet along the coronal loops (see Figure 3) towards the second footpoint and is completely confined within the active region.

In order to understand more about the plasma outflows and the development of the rotation we carried out a line fitting process on the SST/CRISP $H\alpha$ line profiles. Every pixel was fitted with a single, double and triple Gaussian where the χ^2 statistic was minimised to achieve the best fit to the profile. The output was then a structure containing the Gaussian parameters such as centroid wavelength, amplitude and FWHM for each time. For full details on the fitting method please refer to the paper Doyle *et al.* (2019) which describes the methods used and the resulting output in much greater detail. From the output, the centroid wavelengths were used to calculate corresponding Doppler velocities of the line profiles representing upflows and downflows. An example of the velocity map created from these Doppler velocities can be seen in Figure 4(iii) where the map represents an amalgamation of the blue (panel (i)) and red (panel (ii)) wing components detailing the strongest flow movements of the filament/jet plasma. These maps detail the helical nature of the plasma flows where the red represents the plasma falling back to the surface under gravity and the blue the top of the helicity which is being ejected upwards.

3.2. Model

To investigate the details of our event further we utilised a 3D MHD simulation for qualitative comparison with the observed filament eruption and jet. The simulated filament channel progresses in the same way as previous coronal hole jet simulations reported in Wyper *et al.* (2017, 2018). An example of what the model shows can be seen in Figure 4(iv) where the isosurface shows the helical motion of the jet as it propagates away from

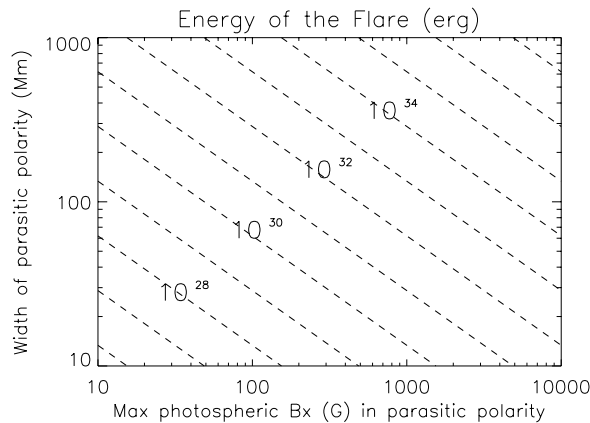


Figure 5. This plot represents a scale up of the solar 3D MHD simulation. The x-axis represent the field strength of the parasitic polarity and the y-axis represent the size of the parasitic polarity. The dashed lines then represent the varying output energies of the flare.

the surface along the coronal loops. Overall, both the observation and the simulation are in good qualitative agreement with each other. For full details of the simulation including the setup conditions and the evolution of the eruption, please refer to Doyle *et al.* (2019).

4. Discussion & Conclusion

In summary, our studies of stellar flares reported in Papers 1 & 2 using one and two-minute photometric data from K2 and TESS we conducted a statistical study on flares in samples of 34 and 149 M dwarfs respectively. Utilising a simple statistical test, we investigated whether the distribution of the flares was random and concluded that none of the stars in the sample showed any preference for certain phase distributions. This was a big surprise, as it indicates other stars do not behave like the Sun where the relationship between solar flares and sunspots is well established.

In a study involving a confined solar flare we used ground-and-space-based observations from SST and SDO and GONG where the event was compared to a 3D MHD simulation. These observations provide the evidence to validate the simulation which can be applied to not only jets and Coronal Mass Ejections but also confined eruptions and flares. Overall, this study explores the finer details of solar flares and their associated eruptive phenomena, providing a unique perspective when applying this knowledge to stellar flare scenarios.

To compare the observations of stellar flares and solar flares the key lies within the 3D MHD simulation. This simulation can be scaled up to see how it would produce flares of greater energies like the ones observed in both low mass and solar-type stars. An example of this scale up can be seen in Figure 5 which shows the conditions needed in both the magnetic strength and size of the parasitic polarity in order to produce flares of greater energies. Overall, our Sun can show flares with energy outputs ranging from 10^{24} - 10^{32} erg. However, studies, like Paper 1 & Paper 2, of low mass and solar-type stars have revealed flares with energies exceeding 10^{32} erg, with ‘superflares’ having energies up to 10^{38} erg (Schaefer *et al.* 2000).

From Figure 5, to produce a flare of energy 10^{34} erg would require a parasitic polarity of size 200Mm and field strength 2kG. For an M dwarf with spectral type M3/M4 this means the active region hosting the parasitic polarity, which may or may not host spots,

would be half the size of the visible stellar disk. In terms of the Sun the field strength of 2kG would be possible as sunspots tend to be in the region of 1kG - 4kG, however a sunspot which is a third of the stellar disk is extremely unlikely. In a study by Aulanier *et al.* (2013), they scaled up their 3D MHD simulation for eruptive flares calculating the parameters needed for larger energy flares. In their highly sheared bipole model, a flare of energy 10^{34} erg would require a bipole the size of 100Mm and field strength of 4kG. Overall, they conclude that solar-type stars which produce superflares with energies $> 10^{33}$ erg would require a much stronger dynamo than the Sun.

References

- Aulanier G., Démoulin P., Schrijver C. J., *et al.* 2013, *A&A*, 549, A66
 Chambers K. C., *et al.* 2016, *arXiv preprint arXiv:1612.05560*
 Davenport J. R. A. 2014, *ApJ*, 797, 122
 Doyle L., Ramsay G., Doyle J. G., Wu K., Scullion E. 2018, *MNRAS*, 480, 2153
 Doyle L., Ramsay G., Doyle J. G., Wu K. 2019, *MNRAS*, 489, 437
 Doyle L., Wyper, P. F., Scullion E., *et al.* 2019, *ApJ*
 Fletcher L., Dennis B. R., Hudson H.S., *et al.* 2011, *Space Science Reviews*, 159, 19
 Gaia Collaboration *et al.* 2016, *A&A*, 595, A1
 Guo J., Lin J., & Deng Y. 2014, *MNRAS*, 441, 2208
 Harvey J., Bolding J., Clark R., *et al.* 2011, *Bulletin of American Astronomical Society*, Vol. 43
 Hawley S. L., Davenport J. R., Kowalski A. F., Wisniewski J. P., *et al.* 2014, *ApJ*, 797, 121
 Karpen J. T., Antiochos S. K., *et al.* 2012, *ApJ*, 760, 81
 Maehara H., *et al.* 2012, *Nature*, 485, 478
 Maehara H., Notsu Y., Notsu S., *et al.* 2017, *PASJ*, 69
 McIntosh P. S. 1990, *Sol. Phys.*, 125, 251
 Pesnell W. D., Thompson B. J. & Chamberlin P. C. 2012, *Sol. Phys.*, 275, 3
 Ricker G. R. *et al.* 2015, *JATIS*, 1, 014003
 Schaefer B. E., King J. R. Deliyannis C. P. 2000, *ApJ*, 529, 1026
 Scharmer G. B., Narayan G., Hillberg T., *et al.* 2008, *ApJ Letters*, 689, L69
 Schmieder B., Demoulin P., & Aulanier G. 2013, *Advances in Space Research*, 51, 1967
 Strassmeier K. G. 1996, *IAU Symposium 176*, p289
 Wolf C. *et al.* 2018, *PASA*, 35, 010
 Wyper P. F., Antiochos S. K. & DeVore C. R. 2017, *Nature*, 544, 452
 Wyper P. F., DeVore C. R. & Antiochos S. K. 2018, *ApJ*, 852, 98
 Young P., & Muglach K. 2014, *Sol Phys.*, 289, 3313

Discussion

KOSOVICHEV: Did you find any stars with a clear solar-like behaviour?

DOYLE: No we did not, in fact all of the stars we have looked at both low mass and solar-type are very un-solar like. Overall they produce much higher energy flares more frequently and all rotate faster than the Sun's 27 day rotation period. It would be interesting to look at stars which have rotation periods similar to the Sun, however, this is a limitation with TESS which has an observation length of ~ 27 days.

MEDINA: Does the rotation period effect whether you see flares at all rotational phases?

DOYLE: No it does not. When we split up our sample in terms of rotation period to check for a presence of rotational phase it makes no difference and we still find the flares are randomly distributed and present at all rotational phases.